



## Modelling correlation between hot working parameters and flow stress of IN625 alloy using neural network

M. Montakhab & P. Behjati

To cite this article: M. Montakhab & P. Behjati (2010) Modelling correlation between hot working parameters and flow stress of IN625 alloy using neural network, Materials Science and Technology, 26:5, 621-625, DOI: [10.1179/174328409X448394](https://doi.org/10.1179/174328409X448394)

To link to this article: <https://doi.org/10.1179/174328409X448394>



Published online: 19 Jul 2013.



Submit your article to this journal [↗](#)



Article views: 22



View related articles [↗](#)



Citing articles: 1 View citing articles [↗](#)

# Modelling correlation between hot working parameters and flow stress of IN625 alloy using neural network

M. Montakhab and P. Behjati\*

In this work, an optimum multilayer perceptron neural network is developed to model the correlation between hot working parameters (temperature, strain rate and strain) and flow stress of IN625 alloy. Three variations of standard back propagation algorithm (Broyden, Fletcher, Goldfarb and Shanno quasi-Newton, Levenberg–Marquardt and Bayesian) are applied to train the model. The results show that, in this case, the best performance, minimum error and shortest converging time are achieved by the Levenberg–Marquardt training algorithm. Comparing the predicted values and the experimental values reveals that a well trained network is capable of accurately calculating the flow stress of the alloy as a function of the processing parameters. Sensitivity analysis revealed that temperature has the largest effect on the flow stress of the alloy being in good agreement with the metallurgical fundamentals.

**Keywords:** Neural network, Superalloy IN625, Flow stress, Hot working

## Introduction

IN625 is a nickel based superalloy that possesses a combination of interesting properties, such as high strength, creep strength, excellent fabricability, weldability and outstanding corrosion resistance,<sup>1</sup> for which it is widely used in aeronautic, aerospace, marine, petrochemical industries and gas turbine engine components. Apart from the fact that strength of the alloy is mainly derived from the stiffening effect of molybdenum and niobium on its nickel chromium matrix, it is observed that precipitation of different phases such as  $M_{23}C_6$ ,  $M_6C$  and  $MC$  carbides,  $\gamma'$ -[ $Ni_3$  (Nb, Al, Ti)],  $Ni_2$ (Cr, Mo) and  $\delta$ -[ $Ni_3$  (Nb, Mo)] occurs on subjecting the alloy to aging treatment in the range of 823–1253 K.<sup>2–8</sup> Since it is required in the wrought form, some investigations have been carried out to elucidate the effect of hot working parameters on final micro-structure and flow stress of the alloy.<sup>9,10</sup> Hot deformation behaviour of materials is always associated with the phenomena, like flow instability, dynamic recovery and dynamic recrystallisation (DRX). Therefore, the correlation between the processing parameters and the final properties is very complex. In fact, an analytical model that quantitatively describes all these relations does not exist.

In this consideration, artificial neural network (ANN) can be used as a powerful technique.<sup>11,12</sup> Artificial neural network can statistically model non-linear functional relationships through a network of nodes or

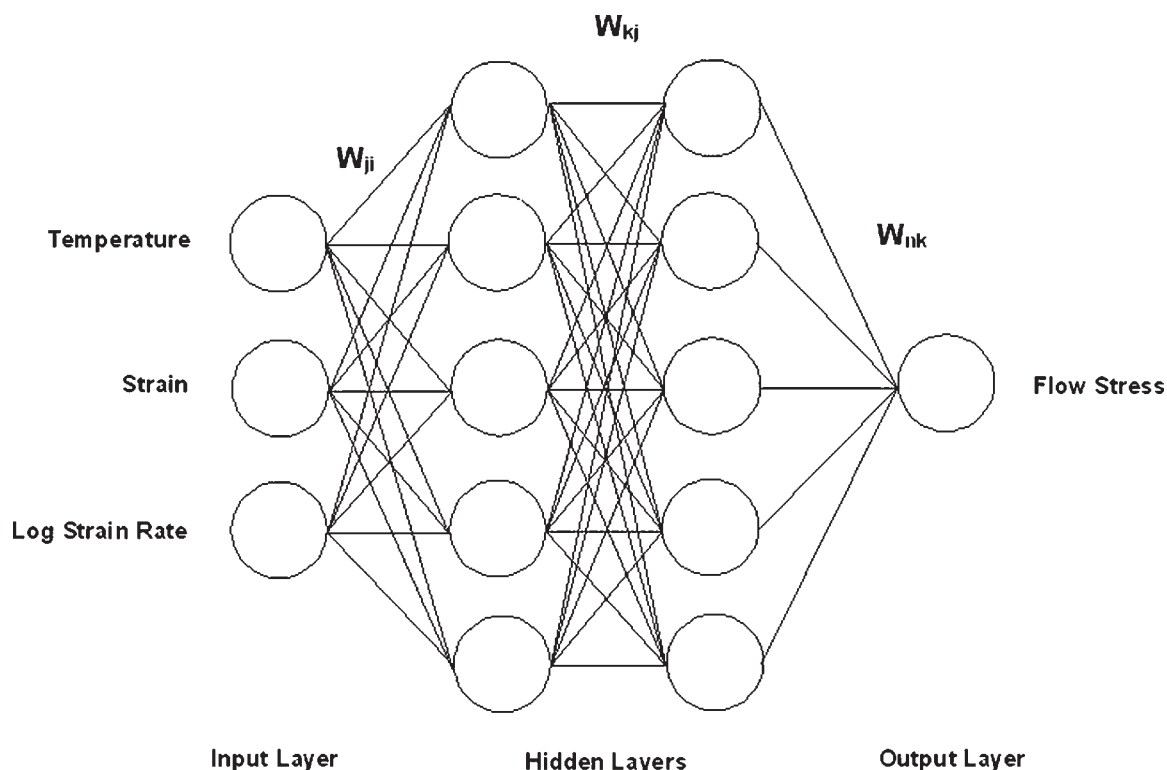
neurons. The nodes are connected together by weighted links. The weights are adjusted through training algorithm and examples. Among the various kinds of existing ANN approaches, the multilayer perceptron (MLP) neural networks have become the most popular in engineering applications. An MLP network generally consists of one input layer, one or more hidden layers and one output layer. The processing units are arranged in layers. Generally, an iterative non-linear optimisation approach using a gradient descent search method is applied to MLP. It provides a feedforward neural network, giving the capacity to capture and represent relationships between patterns in a given data sample. Figure 1 shows the structure of a four-layer feedforward network. Hornik *et al.*<sup>13</sup> showed that this type of network with sigmoid transfer functions, such as *tansig* and *logsig* (Matlab commands), can map any function of practical interest.

The number of nodes in the input and output layers depends on the number of input and output variables respectively. The number of hidden layers and the number of nodes in each hidden layer affects the generalisation capability of the network. Increasing the number of nodes in the hidden layer promotes the accuracy of the model; however, extra nodes may lead to an overfitting in data.<sup>14</sup> The accuracy of MLP network is also affected by the training algorithm used.<sup>15,16</sup> Selection of the suitable training algorithm depends on many factors, including the complexity of the problem, the number of training datasets, the number of weights and biases in the network, the error goal and whether the network is being used for pattern recognition or function approximation.

The back propagation (BP) training algorithm has found widespread use in materials science and

Department of Materials Science and Engineering, Sharif University of Technology, Tehran 11365-8639, Iran

\*Corresponding author, email pbehjati@alum.sharif.edu



1 Structure of a four-layer feedforward network

engineering. Basically, it trains the model by initially assigning a random set of weights and bias values to the network. Presenting the training datasets, these weights and bias values are adjusted with the aim of reducing the corresponding output error. This is repeated for each set of data until the mean square error (MSE) between the predicted output and the desired output reaches a minimum value, it is determined by the equation

$$\text{MSE} = \frac{1}{N} \sum_{k=1}^N [d(k) - O_n(k)]^2 \quad (1)$$

where  $N$  is the number of training datasets ( $N=180$  in this work),  $d$  the desired output of the network and  $O_n$  the predicted output of the network.

In addition to many iterations required for converging, the standard BP algorithm usually does not give an accurate and reliable output. Therefore, a number of variations such as gradient descent BP, gradient descent with adaptive learning rate BP, resilient BP, the Broyden, Fletcher, Goldfarb, and Shanno quasi-Newton (BFG-QN), Levenberg–Marquardt (LM) and Bayesian (BR) have been developed. The latter three algorithms are the most popular and have been used in this investigation. For the sake of brevity, discussing the details of these algorithms is avoided; Refs. 17 and 18 can be consulted to find comprehensive information.

The aim of the present work is to develop an optimum trained ANN to model the correlation between hot working parameters (temperature, strain rate and strain)

and flow stress of IN625 alloy produced by hot extrusion of a powder metallurgy compact.

## Model development

In this work, MLP architecture is used for the modelling purpose. The network has three input parameters (strain rate, temperature and strain) and one output, which is the value of the flow stress. The experimental database used to develop the ANN model has been published by Medeiros *et al.*<sup>10</sup> original reference should be consulted for details of material composition and testing. It includes 210 datasets of which 180 datasets are used for training the network and the remaining 30 datasets are selected randomly to test the performance of the trained network. Testing dataset is not used in the training stage. The range of datasets is given in Table 1.

The output of the  $n$ th node in the output layer  $O_n$  is computed as

$$O_j = f \left( \sum_{i=1}^3 W_{ji} X_i + b_j \right) \quad (2)$$

$$O_k = f \left( \sum_{j=1}^5 W_{kj} O_j + b_k \right) \quad (3)$$

$$O_n = f \left( \sum_{k=1}^5 W_{nk} O_k + b_n \right) \quad (4)$$

Table 1 Range of datasets used in this work

Parameter	Minimum value	Maximum value	Standard deviation
Temperature, °C	900	1200	100
Strain	0.1	0.5	0.141
Strain rate, s <sup>-1</sup>	0.001	100	36.613

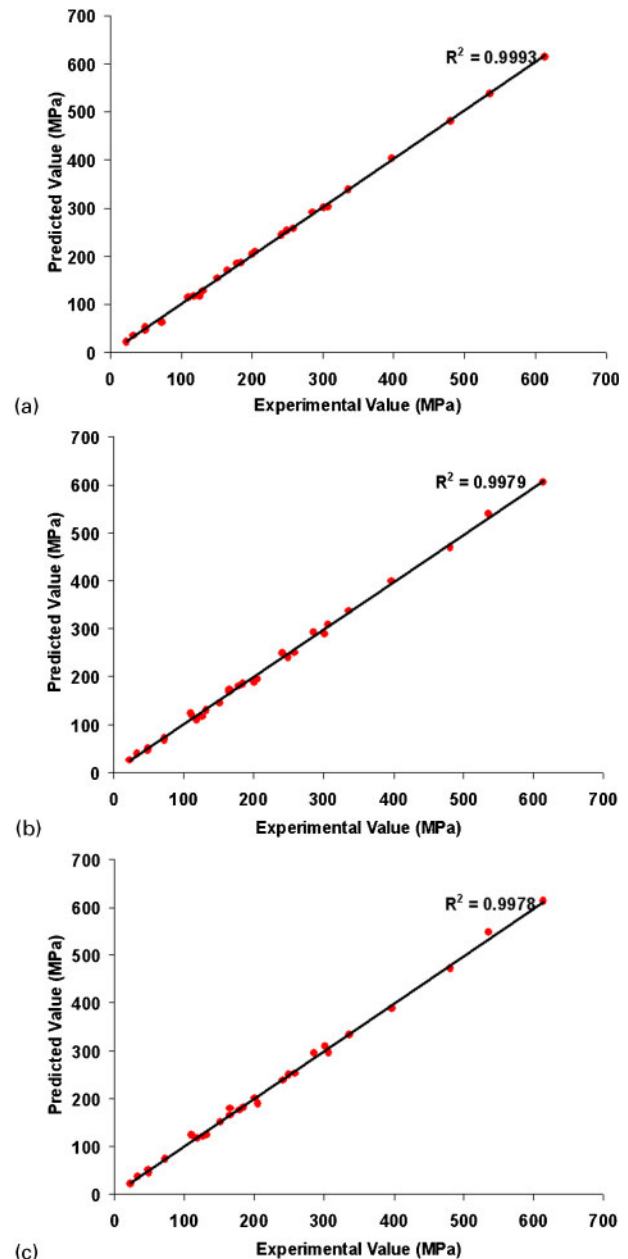
where  $O_j$  and  $O_k$  are the outputs of the  $j$ th and  $k$ th node in the first and second hidden layers,  $X_i$  the input from the  $i$ th node in the input layer,  $W_{ji}$ ,  $W_{kj}$  and  $W_{nk}$  the input/first hidden layer, first hidden layer/second hidden layer and second hidden layer/output layer weights respectively,  $b_j$ ,  $b_k$  and  $b_n$  the bias values of the  $j$ th node,  $k$ th node and  $n$ th node in the first hidden layer, second hidden layer and output layer respectively and  $f$  the transfer function used in each layer.

Before beginning the training process, the input and output values are normalised so that they fall in the range of [0, 1] and [0.2, 0.8] respectively. This normalisation makes the modelling faster and more efficient. The optimum number of the nodes in the hidden layers for each algorithm is achieved through testing a variety of architectures. The corresponding number of iterations required for converging, MSE and correlation coefficient  $R$  are given in Table 2. It is observed that the LM algorithm gives the result with the smaller MSE and in the less number of iterations than those of other algorithms. Therefore, in this case, the LM algorithm is the most suitable algorithm for the network training.

## Results and discussion

Figure 2 represents the performance of the model trained by each algorithm for testing dataset. It is observed that the model values fit the experimental values well. The corresponding number of iterations required for converging and MSE are given in Table 3. It can be seen that the LM algorithm has the smallest error and the least number of iterations. Expectedly,<sup>14</sup> the prediction results for testing dataset have higher error in comparison with training dataset (Table 2).

Figures 3–5 show the combined influence of temperature–strain, temperature–strain rate and strain–strain rates on flow stress of the alloy at different levels of strain, strain rate and temperature. It is observed that, with increase in temperature, flow stress decreases at all strain rates and strains. This can be attributed to the available larger activation energy at higher temperatures, which promotes the dynamic softening arising from DRX. Furthermore, higher thermal energy aids with the activation of more slip systems. With increase in strain, the amount of stored energy and the number of defects within the crystal lattice increase. These promote the formation of new strain free grains during



a LM algorithm; b BR algorithm; c BFG-QN algorithm  
2 Performance of model trained by each algorithm for testing dataset

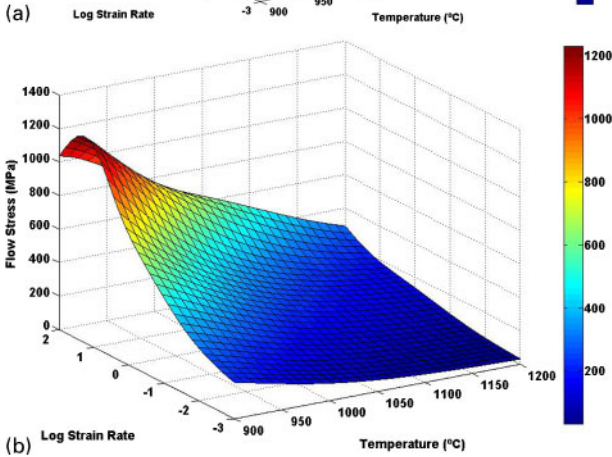
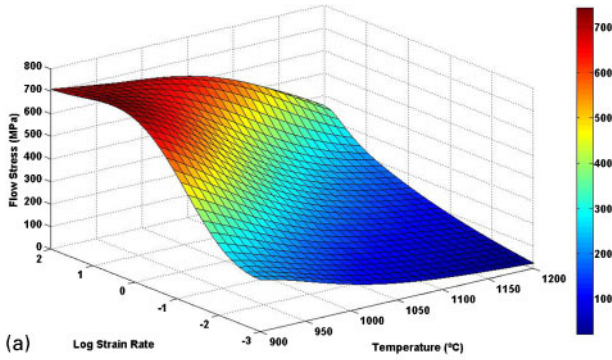
Table 2 Performance of trained network for training dataset

Training algorithm	Number of the nodes in the hidden layer (transfer function)			MSE	Iteration	$R$
	Layer 1	Layer 2	Layer 3			
LM	5 (tansig)	5 (tansig)	0	11.6	3000	0.9999
BR	3 (logsig)	6 (tansig)	3 (logsig)	28.9	2600	0.9998
BFG-QN	8 (tansig)	4 (tansig)	0	33.1	20 000	0.9998

Table 3 Performance of trained network for testing dataset

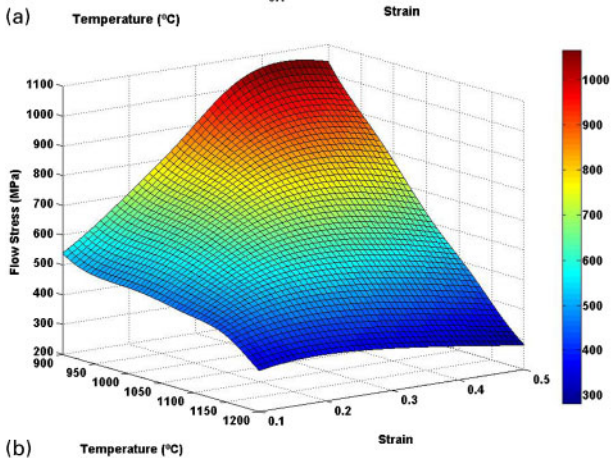
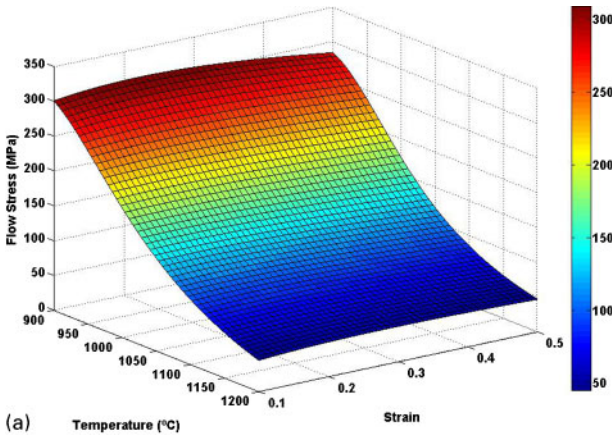
Training algorithm	Number of the nodes in the hidden layer (transfer function)			MSE	Iteration
	Layer 1	Layer 2	Layer 3		
LM	5 (tansig)	5 (tansig)	0	18.0	1800
BR	3 (logsig)	6 (tansig)	3 (logsig)	48.4	1500
BFG-QN	8 (tansig)	4 (tansig)	0	49.8	12 000





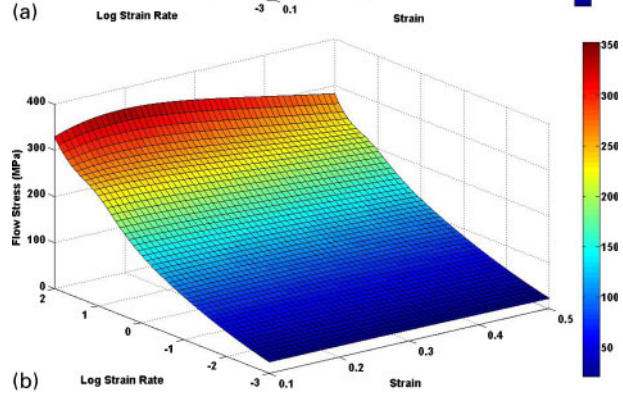
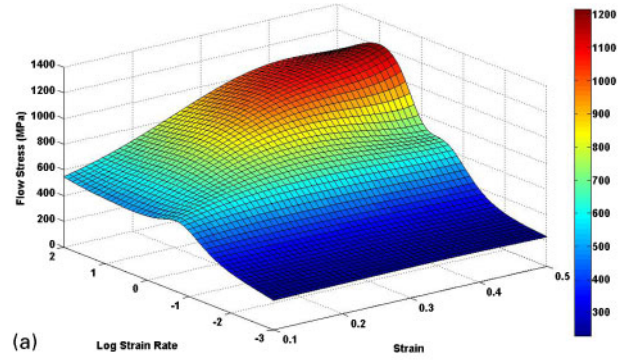
a 0.2; b 0.5

### 3 Combined influence of temperature and strain rate on flow stress of alloy at different strains



a  $0.01 \text{ s}^{-1}$ ; b  $100 \text{ s}^{-1}$

### 4 Combined influence of temperature and strain on flow stress of alloy at different strain rates



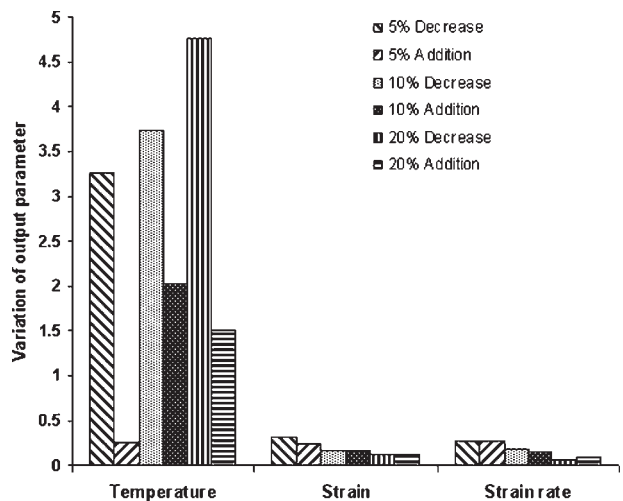
a  $900^\circ\text{C}$ ; b  $1200^\circ\text{C}$

### 5 Combined influence of strain and strain rate on flow stress of alloy at different temperatures

recrystallisation that leads to larger amount of DRX and, consequently, dynamic softening at lower temperatures. On the other hand, with increase in strain rate, flow stress increases due to strain rate hardening.<sup>10,19</sup> Similar behaviour was observed for other levels of parameters and therefore not detailed here.

A sensitivity analysis was carried out on the trained neural network in order to find out the relative importance of the processing parameters. Each of the inputs  $X_k$  was varied at a constant rate. The corresponding percentage change in the output was determined at constant rates of 5, 10 and 20. The sensitivity level  $S_i$  of each input parameter was calculated by the equation

$$S_i(\%) = \frac{1}{N} \sum_{k=1}^N \frac{\% \Delta \sigma_k}{\% \Delta X_k} \times 100 \quad (4)$$



### 6 Relative effect of processing parameters on flow stress of alloy

where  $\sigma$  is the flow stress of the alloy. Figure 6 compares the influence of the temperature, strain and strain rate on the flow stress of the alloy. It is observed that temperature has the largest effect on the flow stress of the alloy. This quantification of relative importance has been found to be supported by metallurgical fundamentals.<sup>10</sup>

## Conclusion

Application of the ANN modelling in this work revealed the following.

1. A well trained network is capable of accurately predicting the flow stress of IN625 alloy as a function of its hot working parameters.

2. Among the different algorithms used for the network training, the LM algorithm gives the result with the smallest MSE and in the least number of iterations.

3. The trained ANN model is capable of simulating the combined influence of processing parameters on the flow stress of alloy.

4. According to the sensitivity analysis, temperature has the largest effect on the flow stress of the alloy, which is consistent with the metallurgical fundamentals.

## References

1. H. L. Eiselstein and D. J. Tillack: 'Superalloys 718, 625 & various derivatives', 1–14; 1991, Warrendale, PA, TMS.
2. M. Sundararaman, P. Mukhopadhyay and S. Baerjee: 'Superalloys 718, 625 & various derivatives', 367–378; 1997, Warrendale, PA, TMS.
3. S. Floreen, G. E. Fuchs and W. J. Yang: 'Superalloys 718, 625 & various derivatives', 13–37; 1994, Warrendale, PA, TMS.
4. C. Vernot-Loier, F. Cortial: 'Superalloys 718, 625 & Various Derivatives', 1991, 409–422.
5. V. Shankar, K. B. Rao and S. L. Mannan: *J. Nucl. Mater.*, 2001, **288**, 222–232.
6. K. M. Chang, H. J. Lai and J. Y. Hwang: 'Superalloys 718, 625 & various derivatives', 683–694; 1994, Warrendale, PA, TMS.
7. L. Ferrer, B. Pieraggi and J. F. Uginet: 'Superalloys 718, 625 & various derivatives', 217–228; 1991, Warrendale, PA, TMS.
8. M. Kohler: 'Superalloys 718, 625 & various derivatives', 363–374; 1991, Warrendale, PA, TMS.
9. D. Zhao, P. K. Chaudhury, R. B. Frank and L. A. Jakman: 'Superalloys 718, 625 & various derivatives', 315–329; 1994, Warrendale, PA, TMS.
10. S. C. Medeiros, W. G. Frazier and Y. V. R. K. Prasad: *Metall. Trans. A*, 2000, **31A**, 2317–2325.
11. S. H. Mousavi Andijan, H. R. Madaah-Hosseini and A. Bahrami: *Mater. Des.*, 2007, **28**, 609–615.
12. A. Bahrami, S. H. Mousavi Andijan and A. Ekrami: *J. Alloys Compd*, 2005, **392**, 177–182.
13. K. Hornik, M. Stinchcombe and H. White: *Neural Networks*, 1989, **2**, (5), 359–366.
14. W. Sha and K. L. Edwards: *Mater. Des.*, 2005, **28**, 1747–1752.
15. Z. Guo and W. Sha: *Comput. Mater. Sci.*, 2004, **29**, (1), 12–28.
16. S. Haykin: 'Neural networks: a comprehensive foundation'; 1999, Upper Saddle River, NJ, Prentice Hall.
17. S. Guessasma and C. Coddet: *Acta Mater.*, 2004, **52**, 5157–5164.
18. R. Koker, N. Altinkok and R. Demir: *Mater. Des.*, 2005, **28**, 1747–1752.
19. S. Mandal, P. V. Sivaprasad and R. K. Dube: *J. Mater. Sci.*, 2007, **42**, 2724–2734.